# A Practical Model for Realistic Butterfly Flight Simulation

QIANG CHEN, Jiangxi University of Finance and Economics, China TINGSONG LU, YANG TONG, and GUOLIANG LUO, East China Jiaotong University, China XIAOGANG JIN, State Key Lab of CAD&CG, Zhejiang University, China ZHIGANG DENG, University of Houston, USA

Butterflies are not only ubiquitous around the world but are also widely known for inspiring thrill resonance, with their elegant and peculiar flights. However, realistically modeling and simulating butterfly flights—in particular, for real-time graphics and animation applications—remains an underexplored problem. In this article, we propose an efficient and practical model to simulate butterfly flights. We first model a butterfly with parametric maneuvering functions, including wing-abdomen interaction. Then, we simulate dynamic maneuvering control of the butterfly through our forcebased model, which includes both the aerodynamics force and the vortex force. Through many simulation experiments and comparisons, we demonstrate that our method can efficiently simulate realistic butterfly flight motions in various real-world settings.

#### CCS Concepts: • Computing methodologies → Procedural animation;

Additional Key Words and Phrases: Computer animation, butterfly animation, aerodynamics, maneuvering control

#### **ACM Reference format:**

Qiang Chen, Tingsong Lu, Yang Tong, Guoliang Luo, Xiaogang Jin, and Zhigang Deng. 2022. A Practical Model for Realistic Butterfly Flight Simulation. *ACM Trans. Graph.* 41, 3, Article 31 (March 2022), 12 pages.

https://doi.org/10.1145/3510459

## 1 INTRODUCTION

Realistic modeling and simulation of living things can find numerous potential applications, including, but not limited to, entertainment, virtual worlds, simulation, education, and so on. In recent

Qiang Chen was supported in part by the Scientific Research Project of Education Department of Jiangxi Province (Grant Nos. GJJ210511, GJJ207109). Guoliang Luo was supported in part by the National Natural Science Foundation of China under Grant 61962021, the Key Research Program of Jiangxi Province under Grant 20202ACBL202008, and the China Postdoctoral Science Foundation under Grant 2020T130264. Xiaogang Jin was supported in part by the National Natural Science Foundation of China (Grant Nos. 62036010, 61972344), and the Ningbo Major Special Projects of the "Science and Technology Innovation" (Grant No. 2020Z007). Zhigang Deng was supported in part by US NSF IIS-2005430. Zhigang Deng was a consulting professor at East China Jiaotong University, China.

Authors' addresses: Q. Chen, Jiangxi University of Finance and Economics, 168 East Shuanggang Rd, Nanchang, Jiangxi, 330013, China; T. Lu, Y. Tong, and G. Luo, East China Jiaotong University, 808 East Shuanggang Rd, Nanchang, Jiangxi, 330013, China; X. Jin, State Key Lab of CAD&CG, Zhejiang University, 866 Yuhangtang Rd, Hangzhou, Zhejiang, 310058, China; Z. Deng (corresponding author), University of Houston, 4800 Calhoun Rd, Houston, Texas, USA, 77204; email: zdeng4@central.uh.edu.

Permission to make digital or hard copies of all or part of this work for personal or classroom use is granted without fee provided that copies are not made or distributed for profit or commercial advantage and that copies bear this notice and the full citation on the first page. Copyrights for components of this work owned by others than the author(s) must be honored. Abstracting with credit is permitted. To copy otherwise, or republish, to post on servers or to redistribute to lists, requires prior specific permission and/or a fee. Request permissions from permissions@acm.org.

© 2022 Copyright held by the owner/author(s). Publication rights licensed to ACM. 0730-0301/2022/03-ART31 \$15.00

https://doi.org/10.1145/3510459

years, various efforts have been made to model and animate a variety of living things, including snakes [Miller 1988], fishes [Hwang et al. 2019; Meng et al. 2018], birds [Ju et al. 2013; Wu and Popović 2003], insects [Wang et al. 2014, 2015], and ants [Xiang et al. 2019].

Butterflies are not only ubiquitous around the world but are also widely known for inspiring thrill resonance with their elegant and peculiar flights. Some previous efforts have been made to quantify and model butterfly flights. For example, researchers studied the principles of butterfly flights through aerodynamics theories, including the unsteady theory that integrates the Computational Fluid Dynamic (CFD) algorithms [Yokoyama et al. 2013]. lso, researchers developed experimentally grounded methods that employ wind tunnel measurements to gauge the aerodynamics for modeling butterflies [Ortega Ancel et al. 2017; Srygley and Thomas 2002]. However, realistically modeling and simulating butterfly flights-in particular, for real-time graphics and animation applications-remains an under-explored problem due to the following: (i) Experimentally based methods have difficulty acquiring the full trajectories and natural body motions of real-world butterflies; (ii) CFD-based methods are impracticable for simulating the motion of butterflies in real time due to their high computational cost; and (iii) unlike many flying insects, a butterfly with charming wings and abdomen can normally fly with small flapping frequencies [Huang and Sun 2012; Sridhar et al. 2016]. Therefore, without taking into account wing-body interaction, it is impossible to simulate the natural and dynamic flight behavior of butterflies in various real-world settings.

In this article, we focus on the efficient simulation of realistic butterfly flights in real-world settings, taking wing-body interaction into consideration. We first model a butterfly with parametric maneuvering functions, including wing-abdomen interaction. Then, we simulate dynamic maneuvering control of the butterfly through our force model, which includes both aerodynamics force and vortex force. Through various simulation experiments and comparisons, we demonstrate that our method can simulate realistic butterfly flight motions in various real-world settings.

The main contributions of this work can be summarized as follows:

- We propose a first-of-its-kind, practical model to simulate butterfly flights with maneuvering functions, which is particularly suitable for real-time graphics and animation applications.
- We introduce a novel force model to simulate the dynamic flight motion of butterflies through both efficient maneuvering control and wing-body interaction modeling.

The remainder of this article is organized as follows. In Section 2, we review the related work on the simulation of flying creatures. We present our schema in Section 3. The details of butterfly modeling and parameters are presented in Section 4. The forces for butterfly flights are explained in Section 5, with detailed descriptions on aerodynamics forces (Section 5.1) and vortex forces (Section 5.2). In Section 6, we describe the details of dynamic maneuvering control. We present our results in Section 7 and discussion and conclusion in Section 8.

#### 2 RELATED WORK

In this section, we briefly review recent related efforts on the simulation of flying creatures. Among the existing works on flying creature simulations, we can roughly divide them into individual flying creature simulations and swarm simulations.

Flying Creature Simulations. Many physically based modeling and simulation approaches were proposed for various flying species, including birds [Ju et al. 2013; Ren et al. 2018; Wu and Popović 2003; Zhu et al. 2006], dragonflies [Isogai et al. 2004; Young et al. 2008], and bats [Pivkin et al. 2005]. Specifically, Wu et al. [2003] apply aerodynamics to animate the bird's wing flapping; they optimize the maneuvering parameters of both the wings and feathers through an offline method. To increase the efficiency and visual quality, Ju et al. [2013] also use the aerodynamics theory to animate realistic bird flights. They first use advanced experimental measurement equipment to capture a real bird's motion and then use the captured data to optimize flight simulations.

In the field of biomechanical simulation, many experimentally based methods [Bode-Oke and Dong 2020; Naranjo 2019; Senda et al. 2012; Slegers et al. 2017; Wang 2005] were proposed for the analysis and simulation of flying insects. For example, Senda et al. [2012] use a wind tunnel to measure the butterfly's aerodynamics forces, which are then used to simulate the wings' flapping. Bode-Oke et al. [2020] simulate the body motion of a monarch butterfly to understand the backward flight kinematics based on the CFD solver. It is noteworthy that although the CFD solver can simulate more accurate wing aerodynamic forces, their method involves heavy computation of the Navier-Stokes equation, which is impracticable for real-time butterfly simulation applications. Dickson et al. [2006] simulate a flying insect as a rigid body. Later, along this line, a few methods were proposed to simulate the butterfly as a rigid body while integrating the abdomen's inertia and moment [Sridhar et al. 2020; Wilson and Albertani 2014]. However, because these methods primarily focus on the wings' and abdomen's oscillations, they generally fall short of generating realistic flight trajectories.

Compared with the existing aerodynamics-based methods (e.g., [Bode-Oke and Dong 2020; Senda et al. 2012]), the main distinctions of our approach include the following. (i) Instead of heavily depending on the computationally expensive CFD solver, our approach directly connects simplified aerodynamic forces with maneuvering functions of the butterfly. (ii) To simulate accurate butterfly body deformation during flights, in addition to introducing a hierarchical skeleton, our approach introduces a new vortex force to simulate the wake influence of wing flapping and generate plausible butterfly motion.

Swarm Simulations. The seminal Boids model [Reynolds 1987] is a simple yet effective technique for animating flocks. However, it does not support physical forces for realistic simulation. By contrast, the bio-inspired flying insect simulation [Wang et al. 2015], mainly based on the three-space model [Couzin et al. 2002], can generate more realistic noisy motions of flying insects. To animate the inherent dynamics of flying insects, Wang et al. [2014] apply a curl-noise field to compute collision-free trajectories for flying insects. In addition, chaotic behavior of flying insects was also extended to generate user-controllable, special effect animations [Chen et al. 2019]. With the recent advances in computer vision techniques, data-driven methods for generating visually plausible animations of flying insects have become increasingly applicable. However, these swarm simulation methods are focused on the macro-level motion of the swarm, that is, generating trajectories of insects in the swarm. For the micro-level motion of individual insects, they often use only cycle-frames (i.e., loop playing of a pre-created sequence) as the individual motion representation.

#### 3 OUR APPROACH

Our approach consists of three main interconnected modules: butterfly modeling, forces computation, and maneuvering control. We give a brief overview on each module here. Figure 1 illustrates the pipeline of our approach. For the sake of clarity, Table 1 lists all of the notations defined in this article along with their descriptions.

Butterfly modeling. We create a butterfly mesh model rigged with a hierarchical skeleton, which is used to animate and control the motion of the butterfly. We also define a set of parametric maneuvering functions to control the wing-abdomen interaction of the butterfly.

Forces computation. In addition to a simplified aerodynamics force for wing deformation, we introduce a vortex force to simulate the wake influence of the wings' flapping. Based on the defined force model, we then control butterfly motion by integrating with attraction targets.

Maneuvering control. We introduce an effective maneuvering control method through body motion decoupling. Based on the computed aerodynamic forces, vortex forces, and attractions from the target, we obtain the velocity of the butterfly. Then, based on the velocity, we further update its body deformation and position. By using a sliding window algorithm, we continuously update maneuvering control parameters to produce smooth and realistic butterfly flight animations.

#### 4 BUTTERFLY MODELING

Without the loss of generality, in this work we construct three-dimensional (3D) models for two butterfly species—the swallowtail butterfly (*Pachliopta aristolochiae*) and monarch butterfly (*Danaus plexippus*)—because of their wide existence on the earth. A swallowtail butterfly flies through flapping the forewings, but a monarch butterfly flies with a trivial difference of the flapping angles between the forewings and the hindwings. Detailed descriptions of the swallowtail and monarch butterflies—including size, mass, chord, and wing area—can be found in existing literature and public databases [Sridhar et al. 2016; Tanaka and Shimoyama 2010], and are summarized in Table 2. In this work, the constructed

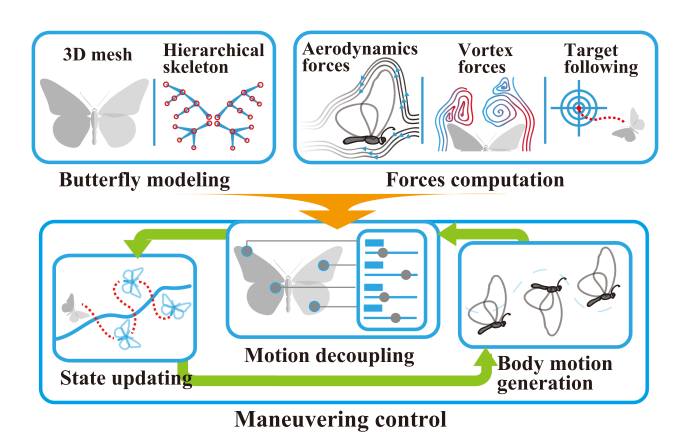


Fig. 1. The pipeline of our approach. First, we construct a butterfly mesh model rigged with a hierarchical skeleton. Then, based on the aerodynamic force and vortex force, we compute the inherent noisy behavior and rapidly adjusted body motion. Finally, we use an efficient maneuvering control method through motion decoupling to generate butterfly body motion and trajectories.

Table 1. The Notations and Their Descriptions in This Article

Notation	Description			
$\theta_{\beta}$	pitch angle of the thorax			
$\theta_{\gamma}$	flapping angle of the wings			
$\theta_{\zeta}$	feathering angle			
$\theta_{\psi}$	sweeping angle			
$\theta_{\phi}$	rotation angle of the abdomen			
$\varphi_a$	amplitude			
f	frequency			
$\varphi_p$	phase angle			
$\varphi_m$	mean angle			
$R_f$	range of the frequency			
$ u^{max} $	max speed of the butterfly			
$R_{\theta_a}$	range of the amplitude			
u	velocity of the butterfly			
p	mass center of the thorax			
a	acceleration of the butterfly			
α	angle of attack			
ρ	air density			
$A_i$	area of the <i>i</i> -th polygon			
V	air velocity over the wing's surface			

monarch 3D model has 11,814 vertices and 23,334 triangles; the swallowtail 3D model has 16,596 vertices and 16,594 triangles. The numbers of the triangles of the wings are 4,132 (swallow-tail butterfly) and 2,096 (monarch butterfly), respectively. Each of the constructed butterfly mesh models consists of five parts: head, thorax, abdomen, forewings, and hindwings, as illustrated in Figure 2.

Based on the Unity Dynamic Bone model [Will 2020], we drive the movement of the butterfly models through a pre-created hierarchical skeleton. Specifically, the thorax is the root that links the forewings, hindwings, and abdomen through the body longitude axis. The skeleton of the butterfly model is depicted in Figure 3.

Table 2. The Wing Areas and Masses of the Body Parts of the Two Selected Butterfly Species

Name	wing area $(10^{-4} m^2)$	Body Mass
Monarch	26	0.428
Swallowtail butterfly	28	0.34

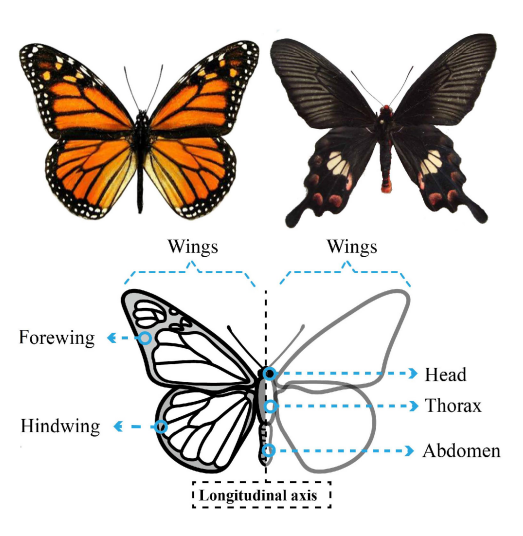


Fig. 2. Schematic illustration of a butterfly's anatomical structure. The topleft is a monarch butterfly, and the top-right is a swallowtail butterfly.

Considering that the deformation of real-world butterfly wings is mainly triggered by the leading edge of the wings (especially the forewings) during flapping, we rig the virtual wing skeleton along the leading edge from the root to the wing tip. In our work, we use two parameters, that is, elasticity and stiffness, to simulate the deformation of the wings and abdomen. In addition to the gravity force, the aerodynamic force (see Section 5.1) as a global force is applied to the root joint when the wings are flapping. Finally, based on the applied forces at each frame, the Dynamic Bone model [Will 2020] can further compute the positions and angles of the skeleton

Generally, the bilateral wings of the butterfly perform flapping with synchronous frequencies [Dudley 2002]. As such, in this work we also treat the butterfly with synchronous frequencies of bilateral wings' flapping motion.

## 4.1 Maneuvering Parameters and Functions

The joint-linked wings of the butterfly flap with a limited range of frequencies and phases. Moreover, according to the findings in Huang and Sun [2012]; Sridhar et al. [2016], a butterfly deforms its abdomen to counteract with wing flapping while flying forward or climbing up/down. To simulate these phenomena, we design the following parameters to model the butterfly's maneuvering.

Parameters for the thorax. The thorax coordinates the wings' flapping through undulating during flights [Kang et al. 2018; Yokoyama et al. 2013]. In our work, we treat the thorax as the root of the butterfly with one Degree of Freedom (DOF). The

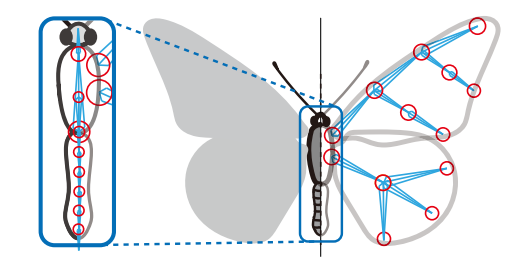


Fig. 3. Illustration of the hierarchical skeleton rigged with a butterfly model in this work.

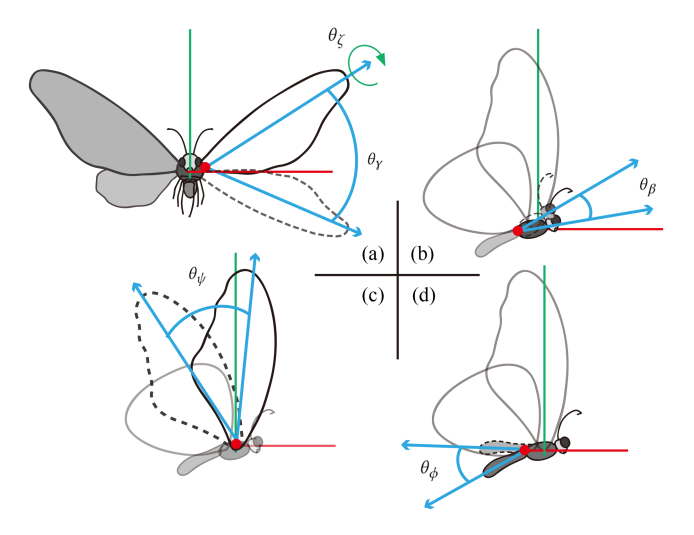


Fig. 4. The abdomen's rotation angle  $\theta_\phi$  and the thorax pitch angle  $\theta_\beta$  are illustrated in (d) and (b), respectively. Using the forewing as an example, the forewing's flapping angle  $\theta_\gamma$  and feathering angle  $\theta_\zeta$  are illustrated in (a), and its sweeping angle  $\theta_\psi$  is illustrated in (c).

controllable parameter for the thorax is denoted as the pitch angle  $\theta_{\beta}$  (see Figure 4(b)).

Parameters for wings. For simplicity, we take the bilateral wings' flapping with synchronous frequencies. Furthermore, in our butterfly model, each fore-wing has 3-DOFs to rotate. Each hind-wing only has 1-DOF for flapping due to its less significant contribution to the flight [Jantzen and Eisner 2008]. The wing-beat parameters include the flapping angle  $\theta_{\gamma}$  for both the fore-wings and the hind-wings (Figure 4(a)), the feathering angle  $\theta_{\zeta}$  for the fore-wings (Figure 4(a)), and the sweeping angle  $\theta_{\psi}$  for the fore-wings (Figure 4(c)).

Parameters for abdomen. The abdomen of the butterfly may visibly rotate along the body longitude axis with the opposite phase to the wings' flapping when it plans to hover, climb up, or move down [Sridhar et al. 2020]. We assign the abdomen with 1 DOF to rotate along the body longitudinal axis.  $\theta_{\phi}$  is defined as the abdomen's rotation angle (Figure 4(d)). To this end, we define  $\chi$  as the set of the above five maneuvering angle parameters:  $\chi = \{\theta_{\mathcal{B}}, \theta_{\mathcal{Y}}, \theta_{\mathcal{Y}}, \theta_{\psi}, \theta_{\phi}\}$ .

To effectively simulate body oscillations, in our work we simplify body undulation as periodical motion. In addition, for the purpose of smooth animation generation, we let the wing flapping

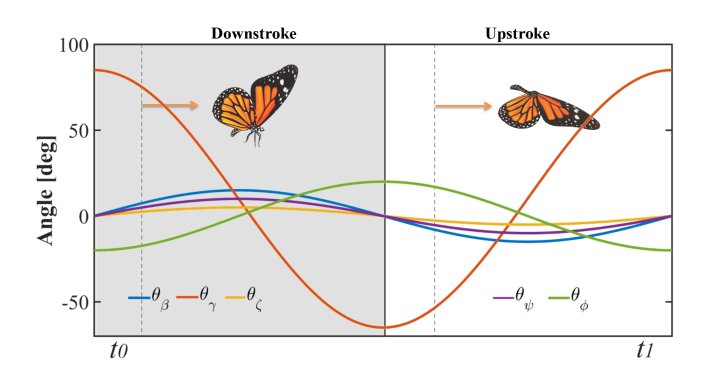


Fig. 5. The phase shifts of the maneuvering angles of the butterfly during one wing flapping cycle (including the upstroke and downstroke of wing flapping).  $t_0$  to  $t_1$  on the X axis denotes the time from the beginning of the downstroke to the end of the upstroke of wing flapping.

motion (wing-beat) during a full cycle start from the highest position to the lowest and then back to the highest position. Let  $t_0$  and  $t_1$  denote the starting and ending time of a flapping cycle, respectively. Then, the maneuvering angles  $\{\theta_\beta, \theta_\gamma, \theta_\zeta, \theta_\psi, \theta_\phi\}$  at a given time t between  $t_0$  and  $t_1$  can be determined through maneuvering functions, described in Equation (1). Figure 5 shows the phase shifts of the five maneuvering angles of the butterfly during a flapping cycle (including the up-stroke and down-stroke).

Inspired by the periodic maneuvering design in Wilson and Albertani [2014]; Wu and Popović [2003], we compute the five maneuvering angles  $\chi = \{\theta_*\}$  as follows:

$$\theta_*(\varphi_a^*(\mathbf{u}), f^*(\mathbf{u}), \varphi_p^*, \varphi_m^*, t) = \varphi_a^*(\mathbf{u}) \cos\left(2\pi f^*(\mathbf{u})t + \varphi_p^*\right) + \varphi_m^*.$$
where  $* \in \{\beta, \gamma, \zeta, \psi, \phi\}$ 

Equation (1) is based on time t and other internal control parameters, including amplitude  $\varphi_a^*(\mathbf{u})$ , which is a function of the butterfly velocity  $\mathbf{u}$ ; frequency  $f^*(\mathbf{u})$ , which is also a function of the butterfly velocity  $\mathbf{u}$ ; the mean value of the angle  $\varphi_m^*$ ; and the phase angle  $\varphi_p^*$ . Both  $\varphi_a^*(\mathbf{u})$  and  $f^*(\mathbf{u})$  can be dynamically adjusted based on the velocity of the butterfly, but the adjustment can be done only across different flapping cycles. This is because, in our work, we assume that the butterfly keeps the frequency parameter f and the amplitude parameter  $\varphi_a$  unchanged within one flapping cycle. The value of  $\varphi_p^*$  is 0 when Equation (1) is used for computing the wing maneuvering parameters (i.e., for computing  $\theta_V$ ,  $\theta_Z$ , and  $\theta_{1/2}$ ), while it is  $-180^{\circ}$  when Equation (1) is used for computing the abdomen maneuvering parameter  $\theta_{\phi}$ , since the abdomen has the opposite phase to the wings' flapping while the butterfly plans to hover, climb up, or move down [Sridhar et al. 2020]. Furthermore,  $\varphi_p^*$  is  $-90^\circ$  when Equation (1) is used for computing the thorax's maneuvering parameter  $heta_{eta}$ .  $\phi_m^*$  remains the same across different flapping cycles.

Since the frequency  $f^*(\mathbf{u})$  in Equation (1) is assumed to be fixed within one flapping cycle, we empirically design and compute  $f^*$  using the butterfly velocity at  $t_0$  as follows:

$$f^*(\mathbf{u}(t_0)) = R_f^* \frac{1}{\left(1 + e^{-16(|\mathbf{u}(t_0)|/|\mathbf{u}^{max}| - 0.5)}\right)}, * \in \{\beta, \gamma, \zeta, \psi, \phi\},$$
(2)

Angle	Parameter Value				
	$R_{f_a}(Hz)$	$R_{\theta_a}$ (°)	$\varphi_p$ (°)	$\varphi_m$ (°)	
$\theta_{\beta}$	0~3	0~30	-90	0	
$\theta_{\gamma}$		0~150	0	10	
$\theta_{\zeta}$	0~11	0~10	-90	0	
$\theta_{\psi}$	0~11	0~20	-90	U	
$\theta_{\phi}$		0~35	-180	-10	

Table 3. Values of Some Parameters Used in Our Experiments

where  $R_f^*$  is the frequency range of the specific maneuvering angle  $\theta_*$ ,  $|\mathbf{u}^{m \dot{a} x}|$  is the maximum flying speed of the butterfly, and  $\mathbf{u}(t_0)$ is the butterfly velocity at time  $t_0$ .

Analogously, we empirically design and compute the amplitude  $\varphi_a^*$  of a maneuvering angle as follows:

$$\varphi_a^*(\mathbf{u}(t_0)) = R_{\theta_a}^* \frac{1}{\left(1 + e^{-16(|\mathbf{u}(t_0)|/|\mathbf{u}^{max}| - 0.5)}\right)}, * \in \{\beta, \gamma, \zeta, \psi, \phi\},$$
(3)

where  $R_{\theta_a}^*$  denotes the amplitude range of the specific maneuvering angle  $\theta_*$ .

In this work, we obtain the maximum flying speed and the ranges of both the frequencies and amplitudes of butterflies from existing biomechanical literature [Kang et al. 2018; Sridhar et al. 2016], which are used in Equations (2) and (3). Specific values of all of the important parameters (including  $\varphi_p^*$ ,  $\varphi_m^*$ ,  $R_{\theta_o}^*$ , and  $R_f^*$ ) used in this work are summarized in Table 3. Note that the parameter values listed in Table 3 may not be perfectly consistent with those of a real butterfly. For example, the flapping frequency of a real monarch butterfly is typically confined to between 9 and 11 Hz [Kang et al. 2018]. However, in our work, we set the range of the flapping frequency to between 0 and 11 Hz. The extra flexibility of the flapping frequency allows us to simulate various butterfly gliding behaviors in virtual worlds.

## FORCES COMPUTATION

During simulations, the instantaneous forces applied onto the butterfly consist of a simplified aerodynamics force on the wings (Section 5.1) and a vortex force on the thorax (Section 5.2).

#### Simplified Aerodynamics Force

Aerodynamics forces originate from the wings' upstroke and downstroke for flying creatures. A butterfly can obtain a lift force from its wings' flapping, and a drag force is caused by air friction. We compute the simplified aerodynamics forces acting on the ith polygon of the butterfly model based on the quasi-state theory [Ellington 1984a]. Thus, the aerodynamic forces can be computed as follows:

$$\mathbf{F}_{i,\text{lift}} = \frac{1}{2}\rho A_i |\mathbf{V}|^2 C_l(\alpha)$$
 and  $\mathbf{F}_{i,\text{drag}} = \frac{1}{2}\rho A_i |\mathbf{V}|^2 C_d(\alpha)$ , (4)

where  $\rho$  is the air density,  $A_i$  is the area of the *i*-th polygon, and **V** is the air velocity over the wing's surface.  $C_l(\alpha)$  and  $C_d(\alpha)$  are the coefficients of the lift force  $\mathbf{F}_{i,lift}$  and the drag force  $\mathbf{F}_{i,drag}$ , respectively. The coefficients  $C_l(\alpha)$  and  $C_d(\alpha)$  are determined by the

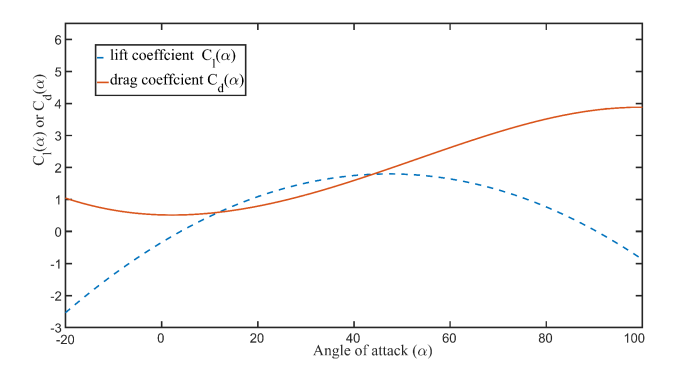


Fig. 6. Relationship between the wing's local angle of attack  $\alpha$  and the coefficients  $C_l(\alpha)$  and  $C_d(\alpha)$ . Lift coefficient function (blue curve):  $-0.0095953\alpha^2 + 0.090635\alpha - 0.34182$ . Drag coefficient function (red curve):  $-0.0000079518\alpha^3 + 0.0011527\alpha^2 + 0.0063148\alpha + 0.51127.$ 

wing's local angle of attack,  $\alpha$ , which can be computed as follows:

$$\alpha = \arctan\left(\frac{|\mathbf{V}^{\mathbf{n}}|}{|\mathbf{V}^{\mathbf{t}}|}\right),\tag{5}$$

where  $V^n$  and  $V^t$  are the components of the air velocity along the normal vector of the wing surface and along the tangent direction (i.e., the vector of base-to-tip), respectively. Figure 6 plots the relationship between the wing's local angle of attack  $\alpha$  and the coefficients  $C_l(\alpha)$  and  $C_d(\alpha)$ . To the best of our knowledge, there are not commonly used Lift/Drag coefficients for butterflies because each kind of flying creature may have different Lift/Drag coefficients. Based on our experiments, we propose empirical Lift/Drag coefficient functions for butterfly flight motion, as shown in Figure 6.

Let  $\mathbf{F}_{i,j} = \mathbf{F}_{i,\text{lift}} + \mathbf{F}_{i,\text{drag}}$  be the resultant aerodynamic force acting on the *i*-th polygon of the *j*-th wing. Then, the instantaneous force  $\mathbf{F}_{j}$  acting on the skeleton from the j-th wing can be computed as follows:

$$\mathbf{F}_{j} = \sum_{i} \mathbf{F}_{i,j}.\tag{6}$$

#### Vortex Force

Many previous research studies confirmed that the leading edge of the wing triggers vortexes and produces a vertical lift force for flying insects [Ellington 1984b; Srygley and Thomas 2002]. However, CFD-based methods that solve the Navier-Stokes equation for vortex simulations are computationally expensive. Furthermore, situations will become more complex if we want to analyze the influence when a dense swarm of flying insects aggregates in the air. In this work, we assume that the fast time variation of vortexes also influences the flight of a butterfly. Moreover, flying insects also present inherent noise behavior, such as tight turn [Betts and Wootton 1988] and vortex-like motion [McInnes 2007].

To simulate the influence of the vortices and the inherent chaotic behavior, we compute an artificial force from a curl-noise field, which is a procedural approach proposed by Bridson et al. [2007] for fluid simulations. By integrating with the Perlin noise [Perlin 2002] to animate the inherent noise behaviors [Betts and Wootton 1988; McInnes 2007], we extend the curl-noise force into low-level simulations as a vortex force acting on the thorax while decoupling the body motion for the butterfly.

The vortex force can be computed as follows:

$$\mathbf{F}_{vor} = \nabla \times \left( \left( s_1 \left( \frac{\mathbf{p}}{gain_x} \right), \ s_2 \left( \frac{\mathbf{p}}{gain_y} \right), \ s_3 \left( \frac{\mathbf{p}}{gain_z} \right) \right) * \eta \right), \tag{7}$$

where  $\mathbf{F}_{vor}$  denotes the vortex force;  $\mathbf{p}$  is the gravity center of the body (thorax);  $s_1$ ,  $s_2$ , and  $s_3$  are the values produced by the Perlin noise function with different noise seeds at  $\mathbf{p}$ ; and gain and  $\eta$  are the parameters used to scale the noise grid density and the magnitude of the Perlin noise, respectively. The parameter gain mainly influences the vortices' shapes: smaller gain values can lead to smaller vortices and vice versa. The parameter  $\eta$  mainly influences the magnitude of the vortex force. In our experiments, we empirically set both  $gain_x$  and  $gain_z$  to 22.0, set  $gain_y$  to 5.5, and set  $\eta$  to 3.66.

Note that this artificial vortex force is used to real-time simulate the wake influence, although it may not be physically accurate. Based on our experiments, we found that when the computed vortex force was directly applied onto the wings, it could lead to excessive twisting on the wings due to both the potentially excessive amplitude and less predictable direction of the vortex force. Thus, we apply the vortex force to the mass center of the thorax of the butterfly only. In our approach, the wing flapping is not *directly* driven by the vortex force. Instead, both the frequency and amplitude of wing flapping are computed based on the velocity (see Equations (2) and (3)) that is dynamically changed by the composite force via acceleration. We will describe how we obtain the acceleration from the vortex force in the next section.

### 6 MANEUVERING CONTROL

In the wild, a real-world butterfly may exhibit peculiar flying styles not only for inherently noisy trajectories but also for rapidly adjusted body motion. It is non-trivial to generate both the inherently noisy trajectories and rapidly adjusted body motion for flying butterflies simultaneously. To achieve this, we decouple the body motion while driving the butterfly by our force model.

#### 6.1 Velocity Computation

To animate the realistic flying motion of the butterfly, we let the butterfly fly towards a given target (e.g., a virtual flower) or let the butterfly follow along a user-specified path. Thus, we can compute a preferred acceleration  $\mathbf{a}_{pre}$  from the given target or a set of user-specified key points that defines a path. However, the butterfly may not strictly hover above the target or follow along a pre-defined global path like a virtual bird in Ju et al. [2013]; Wu and Popović [2003]. Generally, the butterfly endeavors to arrive at a destination, with highly dynamic motion in the process. Further, the butterfly employs its vision to distinguish gender [Li et al. 2017] and sense the environment [Stewart et al. 2015]. Therefore, we design a vision-based algorithm to animate the chaotic motion of the butterfly while it is approaching an attraction target. Its preferred acceleration can be computed as follows:

$$\mathbf{a}_{pre} = R(d) \frac{1}{m} \frac{\mathbf{p} - \mathbf{q}_i}{|\mathbf{p} - \mathbf{q}_i|}, \tag{8}$$

where  $\mathbf{q}_i$  is the closest attraction point,  $\mathbf{p}$  is the gravity center of the butterfly body, m is the mass of the butterfly, and d

 $min(1, |\mathbf{p} - \mathbf{q}_i|/L)$ , L is the maximum sensory length in the field of view (FOV) of the butterfly. The butterfly would not be attracted when its distance to the target was larger than L. FOV acts as the instantaneous sensing space for the butterfly. L is empirically set to 4.5 in our experiments. Also, in Equation (8), we introduce a ramp function R(d) to smoothly cool down its velocity when the butterfly approaches the target. Although different ramp functions could be used, in this work we define R(d) as follows:

$$R(d) = \begin{cases} \frac{15}{8}d - \frac{10}{8}d^3 + \frac{3}{8}d^5, & d \le 1; \\ 0, & \text{otherwise.} \end{cases}$$
 (9)

Our approach drives the butterfly by using both the vortex force and the aerodynamics force in addition to the gravity  $\mathbf{g}$ . Based on Newton's Second Law, we compute the local acceleration  $\mathbf{a}_{loc}$  using the resultant composite force as follows:

$$\mathbf{a}_{loc} = \left(\sum_{j=1}^{4} \mathbf{F}_j + \mathbf{F}_{vor} + \mathbf{g}\right) / m,\tag{10}$$

where  $\sum_{j=1}^{4} \mathbf{F}_{j}$  is the resultant aerodynamics force of all four wings.

Finally, we can obtain the actual acceleration of the butterfly by summing up  $\mathbf{a}_{loc}$  and  $\mathbf{a}_{pre}$ . Let  $\mathbf{u}_{t-1}$  denote the velocity of the butterfly at the previous timestep t-1. Then, we can compute the velocity  $\mathbf{u}_t$  at the current timestep t as follows:

$$\mathbf{u}_t = \mathbf{u}_{t-1} + (\mathbf{a}_{loc} + \mathbf{a}_{pre})\Delta_t. \tag{11}$$

#### 6.2 Maneuvering Update

To generate dynamic motion of the butterfly, we may need to update the values of two internal control parameters, f and  $\varphi_a$ , across different flapping cycles. Recall that, in Section 4.1, we assume that both f and  $\varphi_a$  keep fixed within one flapping cycle, but they can be adjusted before entering into the next cycle.

The drastic change of the frequency or amplitude does not help to save energy during the butterfly's flights [Dudley 1991]. Also, the persistent drastic change of frequency and amplitude will lead to less smooth motion. As such, we need to smooth the values of both f and  $\varphi_a$ . Based on the sliding window algorithm, we use the values of f and  $\varphi_a$  in both previous flapping cycles and the current cycle to compute the parameter values at the next cycle, described here:

$$c_{n+1}^* = 0.5 \left( \sum_{i=max(n-k,1)}^{n-1} w_i c_i^* \right) + 0.5 c_n^*, \text{ where } * \in \{f, \varphi_a\},$$
 (12)

where  $c_n^*$  represents the value of the control parameter \* at the current flapping cycle n, which can be computed using Equations (2) or (3);  $c_{n+1}^*$  represents the value of the control parameter \* used at the next cycle n+1;  $\sum w_i=1$ , and k is the size of the sliding window. In our experiments, k is empirically set to 10.

# 7 RESULTS AND EVALUATIONS

All of the animation results in this article were obtained in the Unity engine. We used our approach to simulate the flights of butterflies in various scenarios and environments, which are reported in Section 7.1. The animation results by our approach can be found in the supplemental demo video.

#### 7.1 Results

We simulated various butterfly flight scenarios, including flying along a user-specified path, interacting with wind, flying in the rain, butterfly chasing, aggregation, and traveling, which are described in this subsection. Note that the aggregation and traveling experiments are mainly used to demonstrate that our approach can be straightforwardly extended for butterfly swarm simulations.

Flying along a user-specified path. A butterfly flying along a user-specified path is commonly seen in simulations or virtual environments. However, unlike birds, a butterfly may not be able to faithfully follow along a given path. Rather, it would display inherently noisy dynamic behavior in this process. As shown in Figures 7 and 8, the body motion and fast undulating of the wings of the simulated butterfly by our approach can be observed. In particular, the wing-abdomen interaction can be clearly observed with a magnified view (Figure 9).

Interacting with wind. Our model can also handle the influence of various external forces on the butterfly during flights, such as wind. Figure 10 shows the motion responses of a flying butterfly when influenced by two different types of wind. As shown in this figure (as well as the demo), the butterfly attempts to recover a stable flight whenever it is influenced by external forces. Also, an interesting spiral trajectory can be observed. When the wind disappears, the butterfly gradually recovers its normal flight

Flying in the rain. To test whether our approach can robustly handle the influence from other environmental factors, we simulated a butterfly flying in the rain. The rain was simulated as particles with varied masses and directions. A spirally falling motion can be observed when the butterfly is hit by the rain, as shown in Figure 11. The animation result of this experiment is provided in the supplemental demo video.

Chasing. We also simulated a scenario in which two virtual butterflies are chasing each other. As shown in Figure 12 (also seen in the demo video), the follower butterfly automatically adjusts its body postures to chase the leader butterfly during the process. It is noteworthy that the simulated butterflies in the chasing example are different butterfly species (i.e., different from the one in Figure 7). From the chasing example as well as additional comparisons (see Section 7.2), we demonstrate that our model can simulate the flight motion of a range of butterflies.

Aggregation. Our model can also be straightforwardly extended to real-time simulate a swarm of butterflies. In the real world, many butterfly species tend to aggregate for migration, such as the monarch. Moreover, a swarm of butterflies can exhibit special visual effects for artistic creation. As shown in Figure 13, we animated more than 100 butterflies using our approach, achieving a real-time speed of 25 frames per second. The macro inherentnoise trajectories of densely aggregated butterflies can be observed. Meanwhile, the body motions of the butterflies were automatically computed according to their flight states. Note that, in this experiment, we did not need to specify a path for each butterfly since the force-driven butterflies fly with chaotic trajectories without collisions. In a sparse scene, collisions can generally be avoided thanks to the divergence-free curl field between any pair of butterflies.

**Traveling.** In addition, we used our approach to simulate a butterfly traveling scenario, as shown in the bottom of Figure 14. The

Table 4. Runtime Statistics of Our Experiments, Including FPS (Frames Per Second) and Computational Time for Two Major Components in Our Approach (Computation of Aerodynamic Force and Computation of Vortex Force)

ID	experiment	# agents	FPS	Aero Force (ms)	Vortex Force
1	along path	1	60	0.41	0.08
2	with wind	1	60	0.46	0.08
3	raining	1	60	0.45	0.08
4	chasing	2	60	0.76	0.14
5	aggregation	100	25	33.69	6.99
6	traveling	200	15	50.56	13.78
7	direct compare	1	60	0.42	0.08

Here "along path" refers to the experiment "flying along a user-specified path" (Figure 9), "with wind" refers to the experiment "interacting with wind" (Figure 10), "raining" refers to the experiment "flying in the rain" (Figure 11), and "direct compare" refer to the experiment "direct comparison with a real butterfly" (Figure 15).

simulated butterflies exhibit various dynamic motions during traveling, such as floating. In this experiment, we also directly compared our simulation result with video footage of real butterflies traveling (see the top of Figure 14). From the comparison, we can see that the simulated butterflies are realistic, and they demonstrate similar dynamic behaviors as those in the wild.

Runtime statistics. We ran all of the simulation experiments of our approach on an off-the-shelf PC with Intel(R) Core(TM) i7-7700 CPU, GeForce RTX 2070 GPU (8G), and 16 GB memory. The simulation performances of our approach are reported in Table 4. Note that our current implementation is unoptimized and does not use any computational power of the GPU. We believe that the simulation efficiency of our approach can be significantly improved if the GPU and code optimization are utilized.

### 7.2 Comparisons

Due to the infeasibility of obtaining ground-truth butterfly flight trajectories (e.g., lack of such publicly shared data for scientific research), we were not able to validate our method through a direct comparison with ground-truth butterfly trajectory data. In addition to an ablation study, in this work we compared our approach with a baseline approach and directly compared our result with video footage of a flying butterfly in the real world, described next.

**Ablation study.** We conducted an ablation study to evaluate the contribution of the vortex force in our force model. In this study, we generated butterfly animations using two conditions: the first was animated by our complete approach and the second was animated by our approach but without the vortex force. As shown in the demo video, the simulated butterfly by our complete approach exhibits inherent-noisy trajectories and realistic wing-abdomen interaction. By contrast, the simulated butterfly without the vortex force loses the dynamics although it still can faithfully fly along a specified path.

Comparison with a baseline approach. In this comparison experiment, we chose the de facto cycle-frames animation method as the baseline approach. The comparison result (refer to the supplemental demo video) demonstrates that our method can generate more realistic butterfly body motion, such as gliding and wingabdomen interaction, than the baseline approach.

Direct comparison with a real butterfly. We also simulated the flying of a single virtual butterfly by directly comparing it with



Fig. 7. A virtual swallow-tail butterfly automatically adjusts its body postures as much as possible while flying along a global path.



Fig. 8. Snapshots of an animated monarch butterfly flying along a given path. It automatically adjusts its body postures during the flight.

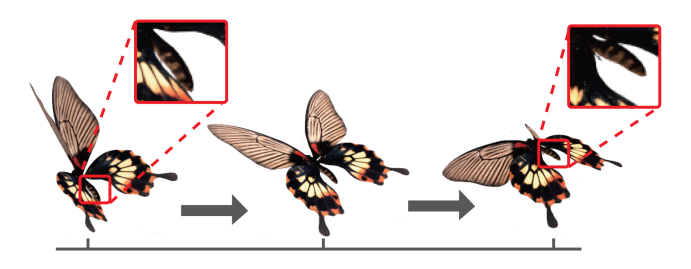


Fig. 9. The simulated wing-abdomen interaction during the flight of a swallow-tail butterfly. The magnified windows show the detailed deformation of the wings and abdomen.

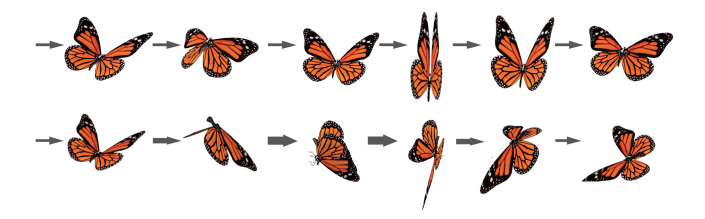


Fig. 10. Our method can simulate a flying butterfly under external force influence. The top row shows snapshots of the butterfly under the influence of a constant wind force. The bottom row shows snapshots of the butterfly under a varying wind force. The direction of the arrow in each snapshot represents the direction of the wind force at that moment, and its width visualizes the strength of the wind force.

a real one from a video. Specifically, we downloaded a butterfly video clip from YouTube.com and then randomly selected a segment of the video as the comparison example. Based on the butterfly in the selected video segment, we manually specified the starting and ending postures of the virtual butterfly, and then used our approach to simulate the rest. All of the maneuvering angles were automatically computed in the simulation process. Finally, we rendered the virtual butterfly into the original video to generate a comparison video. Figure 15 shows a snapshot of the generated comparison video. We can see that during the flight, the wing-abdomen interaction of the virtual butterfly is visually similar to that of the real one. See the demo video for the comparison result.

**Comparisons with different masses.** To study the influence of different masses on butterfly flight simulations, we simulated



Fig. 11. Spirally falling motion can be observed when the butterfly is hit by the rain.



Fig. 12. A snapshot of the simulated butterfly-chasing scenario.

the flights of a virtual butterfly with different masses. During this comparison, we fixed the values of other parameters of a swallow-tail butterfly, except the mass parameter (x 0.5, x 1.0, and x 2.0, respectively). In our approach, the mass can influence the aerodynamics forces and, thus, the acceleration of the butterfly. Also, our simulation results (see the top row of Figure 16 and the supplemental demo video) show that (i) a smaller mass makes the butterfly fly higher due to the lift force and vice versa; and (ii) a larger mass in general makes the butterfly have a higher flapping frequency and amplitude during flights.



Fig. 13. Our method can be extended to animate a virtual swarm of butterflies. As shown in this figure, butterflies in the swarm exhibit various wing-body motions during their flights.





Fig. 14. The butterfly aggregation and traveling result simulated by our approach. The top panel shows a snapshot of a recorded video of traveling monarch butterflies in the wild, while the bottom panel shows the simulation result by our approach.

Comparisons with different scales. To study the effect of wing size on the flights of simulated butterflies (e.g., lift force and drag force), we compared simulated butterflies with different scales. In this comparison, we fixed the values of all other parameters, except the size (scale) of the butterfly model (i.e., x 0.5, x 1.0, and x 1.5, respectively). In our model, the wing area can influence both the lift force and drag force. According to Equation (4), a larger area of the wings will produce larger lift and drag forces. Our simulation results (see the bottom row of Figure 16 and the



Fig. 15. A virtual butterfly is rendered into a video footage with a real butterfly. The right butterfly is the virtual butterfly while the left one is a real butterfly. For the video result, please refer to the supplemental demo video.

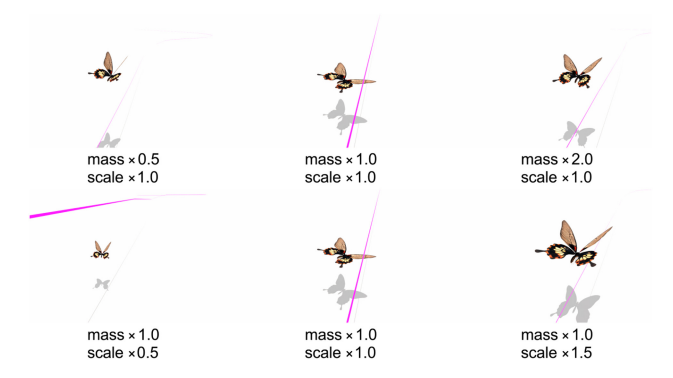


Fig. 16. Comparisons of butterflies with different masses or scales. The top row shows simulated butterflies with different masses. The bottom row shows simulated butterflies with different scales. Basically, a smaller mass makes the butterfly fly higher due to the lift force and vice versa. A virtual butterfly with larger wings can fly higher and produce more instantaneous vertical oscillations.

supplemental demo video) also validate this point. Virtual butterflies with larger wings can fly higher and produce more instantaneous vertical oscillations.

#### 7.3 User Studies

To qualitatively evaluate the simulation results by our approach, we conducted user studies using a 5-point Likert scale. A total of 152 participants, arranged as two groups, were recruited to participate in our user studies. The first group (called Group One) has 107 participants (12 females and 95 males, from 20 to 40 years old). The second group (called Group Two) has 45 participants (16 females and 29 males, from 20 to 37 years old). Most of them are university students in the fields of engineering and computer science, knowing little about computer animation or artistic design.

Realism user study. A total of 7 simulation results (described in Table 4), with ID from 1 to 7, were used as the stimuli in our realism user study. All 107 participants in Group One participated in this study. Each participant can watch each stimulus unlimited times before giving a rating. Before the start of the experiment, the

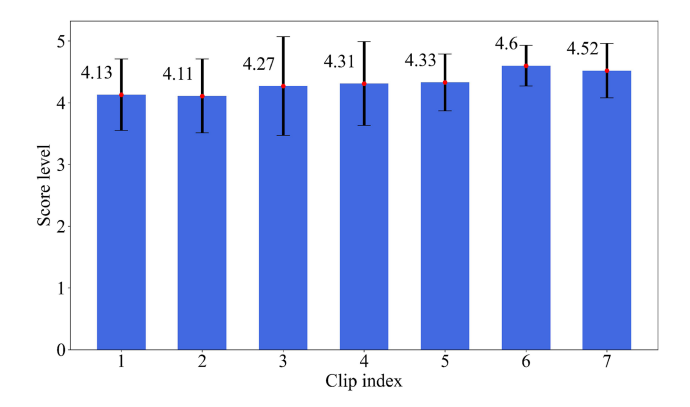


Fig. 17. The average values and variances of all 7 stimuli in our user study. The score variances of the 7 stimuli (clip index from 1 to 7) are 0.59, 0.61, 0.75, 0.60, 0.47, 0.34, and 0.44, respectively. The clip index 1 denotes the "flying along a user-specified path" simulation; clip index 2 denotes the "interacting with wind" simulation; clip index 3 denotes the "flying in the rain" simulation; clip index 4 denotes the "chasing" simulation; clip index 5 denotes the "aggregation" simulation; clip index 6 denotes the "traveling" simulation; and clip index 7 denotes the "direct comparison with a real butterfly" simulation. More details of the 7 stimuli are described in Table 4.

participants were informed that the minimum score 1 denotes "not realistic at all" and the maximum score 5 denotes "super realistic —just like real butterflies." The results of the realism user study are illustrated in Figure 17, where both the average values and the variances of the obtained scores for all stimuli are presented. As shown in this figure, the average score of all of the stimuli is 4.32. Also, the first and second stimuli (i.e., clip index #1 "flying along a userspecified path" and clip index #2 "interacting with wind") received lower scores than the other stimuli. Arguably, the main reason is that, in the first two simulations, the butterfly was rendered without any background environment (i.e., a pure white background), which may affect the participants' visual perception of the butterfly. By contrast, the #6 and #7 stimuli, which denote the swam "traveling" simulation and the "direct comparison with a real butterfly" simulation, respectively, received high average scores and low variances. This realism study validates that our approach can generate realistic butterfly flight motion in various real-world settings.

To analyze the reliability of the received user ratings in this realism study, we use Cronbach's alpha ( $\alpha^c$ ) as a coefficient to test internal consistency. It can be computed as follows:

$$\alpha^{c} = \left(\frac{n}{n-1}\right) \left(\frac{\sigma^{2} - \sum \sigma_{i}^{2}}{\sigma^{2}}\right),\tag{13}$$

where  $\sigma^2$  denotes the total variance, n is the total number of the used stimuli, and  $\sigma_i^2$  denotes the score variance of the i-th stimulus. The score variances of all 7 stimuli are shown in Figure 17. The computed total variance is 11.61. The computed Cronbach's alpha  $\alpha^c$  is 0.78. Note that  $\alpha^c > 0.7$  is generally considered as an acceptable threshold for internal consistency.

In addition, after the study, we asked the participants to send us their free-form opinions on "what is the main visual difference between a simulated butterfly and a real one." We received a total of 15 responses, most of which mention that the main visual

Table 5. Average Values, Variances, and Statistical Test Results of the User Scores Obtained in the Validation User Study

EXPER	Method	sco	ores	F-ratio	p-value
EAFER		Average	Variance	r-ratio	
Baseline	BL	2.02	0.57	260.6	<0.01
	ours	4.49	0.48		
Ablation	w/o VF	1.93	0.56	297.9	<0.01
	ours	4.44	0.39		

"Baseline" in the EXPER column refers to the "comparison with a baseline approach" experiment (in Section 7.2). In the Baseline row, "BL" in the method column denotes the baseline approach and "ours" denotes our method. "Ablation" in the EXPER column refers to the "Ablation study" experiment. In the ablation row, "w/o VF" denotes our method without vortex force, and "ours" denotes our complete method.

difference is the subtle softness and weaving motion effect on the butterfly wings' surface. This shows that there is still room for further improving the visual realism of simulated butterfly flights.

Validation user study. We also conducted a validation user study to evaluate the 2 simulation results from the baseline comparison experiment (see Section 7.2) and the 2 simulation results from the ablation study experiment (see Section 7.2). All 45 participants in Group Two participated in this study. Just like in the already discussed realism study, participants were asked to give a score from 1 (not realistic at all) to 5 (just like real butterflies) for each watched simulation. As shown in Table 5, our method received a higher average score than the baseline method, and the scores of the ablation study clips indicate that the introduced vortex force in our model helps to produce more realistic butterfly flight motion. We used the ANOVA method to compute the p-values for the two comparisons (reported in Table 5). The computed p-values of the two comparisons are smaller than 0.01, which means that there are statistically significant differences between the two stimuli in each of the comparison pairs, that is, between the baseline method and our method, and between the ablation study version (without vortex force) and our complete approach.

#### 8 DISCUSSION AND CONCLUSION

In this article, we present a practical approach to efficiently simulate butterfly flights in various real-world settings. We introduce a force-based model, including a simplified aerodynamic force and a vortex force, to animate the fast undulating of wing-abdomen interaction during butterfly flights. We also introduce motion decoupling into the maneuvering control of the flying butterfly. Through experiments, comparisons, and user studies, we demonstrate that our model can real-time generate realistic butterfly flight animations for a variety of scenarios.

Despite the demonstrated effectiveness, our current method has several limitations, described here.

Our current approach can simulate the wing-abdomen interaction of the butterfly. However, it does not include the simulation of butterfly take-off and landing motions, which may need certain types of coordination between the legs and the body. Based on our observation, insects may obtain momentum from both the wings flapping and the legs jumping. Furthermore, the butterfly may not simply apply

- lift force to obtain the thrust through the downstroke during a take-off motion [Johansson and Henningsson 2021]. This could be different from the normal flight state, in which the butterfly obtains lift force through downstrokes.
- The maneuvering functions in our current approach are mostly inspired by existing biological and biomechanical literature. Due to the practical difficulty and challenge of acquiring ground-truth motion (in particular, both wing motion and body motion) of butterflies in natural outdoor environments, we are not able to obtain such data for our model calibration or training. Therefore, the simulated motion by our current approach may not be perfectly aligned with real butterflies in the natural world, although it is practical and efficient to generate visually compelling simulations.
- The skeleton-driven body deformation in our current approach is insufficient to produce the subtle softness and weaving motion effects often observed on the wings of a real butterfly. Advanced deformation and simulation algorithms (e.g., physically accurate modeling algorithms) need to be designed to achieve such subtle simulations. We also observe that the weaving motion of butterfly wings often propagates from the root to the wing tip, from the leading edge to the opposite edge, and from the forewings to the hindwings. Therefore, to simulate realistic weaving motion observed on the butterfly wings, we need to computationally model the relationship between the forces acted on the wings and weaving motion.

As future work, we plan to build an in-house motion acquisition setup to acquire accurate motion of butterflies in indoor settings. Then, we will utilize such data to calibrate our model or develop new data-driven approaches to accurately model and animate virtual butterflies. Also, we plan to develop novel algorithms to simulate the landing and take-off motions of butterflies in virtual environments.

#### REFERENCES

- C. R. Betts and R. J. Wootton. 1988. Wing shape and flight behaviour in butterflies (Lepidoptera: Papilionoidea and hesperioidea): A preliminary analysis. Journal of Experimental Biology 138, 1 (1988), 271-288.
- Ayodeji T. Bode-Oke and Haibo Dong. 2020. The reverse flight of a monarch butterfly (Danaus plexippus) is characterized by a weight-supporting upstroke and postural changes. Journal of the Royal Society Interface 17, 167 (2020), 20200268
- Robert Bridson, Jim Houriham, and Marcus Nordenstam. 2007. Curl-noise for procedural fluid flow. ACM Transactions on Graphics 26, 3 (2007), 46-es.
- Qiang Chen, Guoliang Luo, Yang Tong, Xiaogang Jin, and Zhigang Deng. 2019. Shapeconstrained flying insects animation. Computer Animation and Virtual Worlds 30, 3-4 (2019), e1902.
- Iain D. Couzin, Jens Krause, Richard James, Graeme D. Ruxton, and Nigel R. Franks. 2002. Collective memory and spatial sorting in animal groups. Journal of Theoretical Biology 218, 1 (2002), 1-11.
- William Dickson, Andrew Straw, Christian Poelma, and Michael Dickinson. 2006. An integrative model of insect flight control. In 44th AIAA Aerospace Sciences Meeting and Exhibit, Reno, Nevada, Jan 9-12, 2006. AIAA publisher, 34 pages.
- Robert Dudley. 1991. Biomechanics of flight in neotropical butterflies: Aerodynamics and mechanical power requirements. Journal of Experimental Biology 159, 1 (1991), 335-357.
- Robert Dudley. 2002. The Biomechanics of Insect Flight: Form, Function, Evolution. Princeton University Press.
- Charles Porter Ellington. 1984a. The aerodynamics of hovering insect flight. I. The quasi-steady analysis. Philosophical Transactions of the Royal Society of London. B, Biological Sciences 305, 1122 (1984), 1-15.
- Charles Porter Ellington. 1984b. The aerodynamics of hovering insect flight. V. A vortex theory. Philosophical Transactions of the Royal Society of London. B, Biological Sciences 305, 1122 (1984), 115-144.

- Hua Huang and Mao Sun. 2012. Forward flight of a model butterfly: Simulation by equations of motion coupled with the Navier-Stokes equations. Acta Mechanica Sinica 28, 6 (2012), 1590-1601.
- Yura Hwang, Theodore A. Uyeno, and Shinjiro Sueda. 2019. Bioinspired simulation of knotting hagfish. In International Symposium on Visual Computing, volume 11844, Lake Tahoe, Nevada/California, October 2019. Springer, 75–86.
- Koji Isogai, Shun Fujishiro, Taku Saitoh, Manabu Yamamoto, Masahide Yamasaki, and Manabu Matsubara. 2004. Unsteady three-dimensional viscous flow simulation of a dragonfly hovering. AIAA Journal 42, 10 (2004), 2053-2059.
- Benjamin Jantzen and Thomas Eisner. 2008. Hindwings are unnecessary for flight but essential for execution of normal evasive flight in Lepidoptera. Proceedings of the National Academy of Sciences 105, 43 (2008), 16636-16640.
- L. C. Johansson and P. Henningsson. 2021. Butterflies fly using efficient propulsive clap mechanism owing to flexible wings. Journal of the Royal Society Interface 18, 174 (2021), 20200854.
- Eunjung Ju, Jungdam Won, Jehee Lee, Byungkuk Choi, Junyong Noh, and Min Gyu Choi. 2013. Data-driven control of flapping flight. ACM Transactions on Graphics 32, 5 (2013), 1-12.
- Chang-kwon Kang, Jacob Cranford, Madhu K. Sridhar, Deepa Kodali, David Brian Landrum, and Nathan Slegers. 2018. Experimental characterization of a butterfly in climbing flight. AIAA Journal 56, 1 (2018), 15-24.
- Chengzhe Li, Hua Wang, Xiaoming Chen, Jun Yao, Lei Shi, and Chengli Zhou. 2017. Role of visual and olfactory cues in sex recognition in butterfly Cethosia cyane cyane. Scientific Reports 7, 1 (2017), 1-9.
- Colin R. McInnes. 2007. Vortex formation in swarms of interacting particles. Physical Review E 75, 3 (2007), 032904.
- Xiangfei Meng, Junjun Pan, Hong Qin, and Pu Ge. 2018. Real-time fish animation generation by monocular camera. Computers & Graphics 71 (2018), 55-65.
- Gavin S. P. Miller. 1988. The motion dynamics of snakes and worms. In ACM SIG-GRAPH Computer Graphics 22, 4 (1998), 169-173.
- Steven E. Naranjo. 2019. Assessing insect flight behavior in the laboratory: A primer on flight mill methodology and what can be learned. Annals of the Entomological Society of America 112, 3 (2019), 182-199.
- Alejandro Ortega Ancel, Rodney Eastwood, Daniel Vogt, Carter Ithier, Michael Smith, Rob Wood, and Mirko Kovač. 2017. Aerodynamic evaluation of wing shape and wing orientation in four butterfly species using numerical simulations and a lowspeed wind tunnel, and its implications for the design of flying micro-robots. Interface Focus 7, 1 (2017), 20160087,
- Ken Perlin. 2002. Improving noise. ACM Transactions on Graphics 21, 3 (2002), 681-
- Igor V. Pivkin, Eduardo Hueso, Rachel Weinstein, David H. Laidlaw, Sharon Swartz, and George E. Karniadakis. 2005. Simulation and visualization of air flow around bat wings during flight. In International Conference on Computational Science, Atlanta, GA, May 22-25, 2005. Springer, 689-694.
- $Jiaping\,Ren, Wanxuan\,Sun, Dinesh\,Manocha, Aming\,Li, and\,Xiaogang\,Jin.\,2018.\,Stable$ information transfer network facilitates the emergence of collective behavior of bird flocks. Physical Review E 98, 5 (2018), 052309.
- Craig W. Reynolds. 1987. Flocks, herds and schools: A distributed behavioral model. In ACM SIGGRAPH Computer Graphics 21, 4 (July 1987), 25-34.
- Kei Senda, Takuya Obara, Masahiko Kitamura, Tomomi Nishikata, Norio Hirai, Makoto Iima, and Naoto Yokoyama. 2012. Modeling and emergence of flapping flight of butterfly based on experimental measurements. Robotics and Autonomous Systems 60, 5 (2012), 670-678.
- Nathan Slegers, Michael Heilman, Jacob Cranford, Amy Lang, John Yoder, and Maria Laura Habegger. 2017. Beneficial aerodynamic effect of wing scales on the climbing flight of butterflies. Bioinspiration & Biomimetics 12, 1 (2017), 016013.
- Madhu Sridhar, Chang-Kwon Kang, and D. Brian Landrum. 2016. Instantaneous lift and motion characteristics of butterflies in free flight. In 46th AIAA Fluid Dynas ics Conference, Washington, D.C., June 13 - 17, 2016. AIAA publisher, 3252.
- Madhu Sridhar, Chang-Kwon Kang, and Taeyoung Lee. 2020. Geometric formulation for the dynamics of monarch butterfly with the effects of abdomen undulation. In AIAA Scitech 2020 Forum, Orlando, FL, Jan 6-10, 2020. AIAA publisher, 1962.
- R. B. Srygley and A. L. R. Thomas. 2002. Unconventional lift-generating mechanisms in free-flying butterflies. Nature 420, 6916 (2002), 660-664
- Finlay J. Stewart, Michiyo Kinoshita, and Kentaro Arikawa. 2015. The roles of visual parallax and edge attraction in the foraging behaviour of the butterfly Papilio xuthus. Journal of Experimental Biology 218, 11 (2015), 1725–1732.
- H. Tanaka and I. Shimoyama. 2010. Forward flight of swallowtail butterfly with simple flapping motion. Bioinspiration & Biomimetics 5, 2 (2010), 026003.
- Xinjie Wang, Xiaogang Jin, Zhigang Deng, and Linling Zhou. 2014. Inherent noiseaware insect swarm simulation. In Computer Graphics Forum, Vol. 33. Wiley Online Library, 51-62.
- Xinjie Wang, Jiaping Ren, Xiaogang Jin, and Dinesh Manocha. 2015. BSwarm: Biologically-plausible dynamics model of insect swarms. Proceedings of the 14th ACM SIGGRAPH/Eurographics Symposium on Computer Animation, Los Angeles, CA, August 7-9, 2015. 111-118.
- Z. Jane Wang. 2005. Dissecting insect flight. Annual Review of Fluid Mechanics 37 (2005), 183-210.

- Hong Will. 2020. Dynamic bone. National Harbor, Maryland, USA, Jan 13-17, 2014.
  AIAA Publisher. Retrieved February 7, 2022 from https://assetstore.unity.com/packages/tools/animation/dynamic-bone-16743.
- Tyler Wilson and Roberto Albertani. 2014. Wing-flapping and abdomen actuation optimization for hovering in the butterfly Idea leuconoe. In 52nd Aerospace Sciences Meeting. ACM Press, 0009.
- Jia-chi Wu and Zoran Popović. 2003. Realistic modeling of bird flight animations. ACM Transactions on Graphics 22, 3 (2003), 888–895.
- Wei Xiang, Jiaping Ren, Kuan Wang, Zhigang Deng, and Xiaogang Jin. 2019. Biologically inspired ant colony simulation. Computer Animation and Virtual Worlds 30, 5 (2019), e1867.
- Naoto Yokoyama, Kei Senda, Makoto Iima, and Norio Hirai. 2013. Aerodynamic forces and vortical structures in flapping butterfly's forward flight. *Physics of Fluids* 25, 2 (2013), 4191–4208.
- John Young, Joseph C. S. Lai, and Charly Germain. 2008. Simulation and parameter variation of flapping-wing motion based on dragonfly hovering. AIAA Journal 46, 4 (2008), 918–924.
- Chaojiang Zhu, Kazunobu Muraoka, Takeyuki Kawabata, Can Cao, Tadahiro Fujimoto, and Norishige Chiba. 2006. Real-time animation of bird flight based on aerodynamics. The Journal of the Society for Art and Science 5, 1 (2006), 1–10.

Received August 2021; revised December 2021; accepted January 2022